Iterative image reconstruction using prior knowledge

Hsin M. Shieh

Department of Electrical Engineering, Feng Chia University, 100 Wenhwa Road, Seatwen, Taichung, Taiwan 40724

Charles L. Byrne

Department of Mathematical Sciences, University of Massachusetts Lowell, One University Avenue, Lowell, Massachusetts 01854

Markus E. Testorf

Thayer School of Engineering, Dartmouth College, 8000 Cummings Hall, Hanover, New Hampshire 03755

Michael A. Fiddy

Center for Optoelectronics and Optical Communications, The University of North Carolina at Charlotte, 9201 University City Boulevard, Charlotte, North Carolina 28223

Received August 12, 2005; accepted November 18, 2005; posted January 10, 2006 (Doc. ID 64112)

A method is proposed to reconstruct signals from incomplete data. The method, which can be interpreted both as a discrete implementation of the so-called prior discrete Fourier transform (PDFT) spectral estimation technique and as a variant of the algebraic reconstruction technique, allows one to incorporate prior information about the reconstructed signal to improve the resolution of the signal estimated. The context of diffraction tomography and image reconstruction from samples of the far-field scattering amplitude are used to explore the performance of the method. On the basis of numerical computations, the optimum choice of parameters is determined empirically by comparing image reconstructions of the noniterative PDFT algorithm and the proposed iterative scheme.

OCIS codes: 100.3010, 100.3020, 100.3190, 100.6640, 100.6950.

1. INTRODUCTION

A large number of inverse problems can be described as computing the image of an object from samples of its Fourier transformation. This includes computerized tomography, diffraction tomography, many variants of radar-imaging applications, and the estimate of spectra from a finite time series.

A significant problem in reconstructing an image $f(\mathbf{r})$ from finitely many projections is the limited nature of the data, allowing for nonunique solutions. The prior discrete Fourier transform (PDFT) method[1–6] incorporates prior information about the image, such as support information or profile information, through the use of a weight function $p(\mathbf{r}) \geqslant 0$. The image obtained with the PDFT is a data-consistent member of a finite-parameter family of functions of a continuous variable $\mathbf{r}$. There are as many parameters as there are data values, and the parameters are determined from the data when a system of linear equations is solved. The matrix involved in this system comes from the weight function $p(\mathbf{r})$. The term PDFT denotes the PDFT estimator in the case of Fourier transform data, where the image is computed as a product of the prior $p(\mathbf{r})$ and a discrete Fourier transformation. However, we emphasize that the PDFT is not limited to this problem but can be applied to any data set that can be interpreted as projections in a Hilbert space that describes the experimental geometry.

Suppose $g_m(\mathbf{r})$, for $m = 1, 2, \ldots, M$, are known functions and the data vector $\mathbf{d}$ has the entries

$$d_m = \int f(\mathbf{r})\overline{g_m(\mathbf{r})}\mathrm{d}\mathbf{r}. \tag{1}$$

For $n = 1, 2, \ldots, M$, let $\mathbf{P}$ be the square matrix with entries

$$P_{mn} = \int p(\mathbf{r})g_n(\mathbf{r})\overline{g_m(\mathbf{r})}\mathrm{d}\mathbf{r}, \tag{2}$$

and let the vector $\mathbf{a}$ satisfy the system $\mathbf{d} = \mathbf{Pa}$. Then the PDFT estimate of the image function $f(\mathbf{r})$ is

$$\hat{f}_{PDFT}(\mathbf{r}) = p(\mathbf{r})\sum_{n=1}^{M} a_n g_n(\mathbf{r}). \tag{3}$$

The cumbersome part of using the PDFT is usually the formation of the matrix $\mathbf{P}$, particularly when M is large. Our purpose, in this paper, is to illustrate how to avoid the use of this matrix. The following fact about the PDFT is the basis for our new method.

The PDFT estimate of $f(\mathbf{r})$ is the function consistent with the data whose weighted norm is minimized, where the squared weighted norm of a function $h(\mathbf{r})$ is defined to be

$$\|h\|^2 = \int |h(\mathbf{r})|^2 p^{-1}(\mathbf{r}) \mathrm{d}\mathbf{r}. \tag{4}$$

It follows from the theory of Hilbert space that the PDFT estimate must have the form of Eq. (3).

The discrete PDFT (DPDFT) uses discrete representations of $f(\mathbf{r})$ and $p(\mathbf{r})$ represented by finite N by 1 vectors $\mathbf{f}$ and $\mathbf{p}>0$, with $N>M$. The integration in Eq. (1) is replaced by a summation. We have

$$d_m = \sum_{n=1}^{N} A_{mn} f_n, \tag{5}$$

with $m=1,\ldots,M$.

Vector $\mathbf{f}$ is the discrete image estimate, which satisfies $\mathbf{d}=\mathbf{Af}$, and for which the squared weighted norm reads as

$$\|\mathbf{f}\|_p^2 = \sum_{n=1}^{N} |f_n|^2/p_n. \tag{6}$$

In closed form the minimum weighted norm solution is given by

$$\hat{\mathbf{f}}_{DPDFT} = \mathbf{W}^{-1}\mathbf{A}^{\dagger}(\mathbf{A}\mathbf{W}^{-1}\mathbf{A}^{\dagger})^{-1}\mathbf{d}, \tag{7}$$

where $\mathbf{W}$ is the diagonal matrix having the entries $1/p_n$ on the diagonal. Using the closed form to calculate the solution is not efficient for large data sets. Instead, we calculate the DPDFT solution using the algebraic reconstruction technique[7–12] (ART). For the remainder of this paper we shall be concerned with the case of Fourier transform data.

The main contribution of this paper is to demonstrate that the cumbersome aspects of the PDFT can be avoided through the DPDFT, without degrading the image resolution. It is true that, in certain cases, the matrix $\mathbf{P}$ may exhibit a special structure, such as being Toeplitz or block Toeplitz, and this structure can be exploited to obtain fast inversion schemes. Nevertheless, it is the actual computation of $\mathbf{P}$ that we wish to avoid.

2. DISCRETE PRIOR DISCRETE FOURIER TRANSFORM

We consider the problem of estimating $f(\mathbf{r})$ from finitely many Fourier transform values, $F(\mathbf{k}_m)$ for $m=1,2,\ldots,M$. The PDFT estimator is given by

$$\hat{f}_{PDFT}(\mathbf{r}) = p(\mathbf{r}) \sum_{m=1}^{M} a_m \exp(j\mathbf{r}\cdot\mathbf{k}_m), \tag{8}$$

where $p(\mathbf{r}) \geqslant 0$ is the prior function. The coefficients a_m for $m=1,2,\ldots,M$ satisfy the matrix equation

$$\mathbf{d} = \mathbf{Pa}, \tag{9}$$

where $\mathbf{d}=[F(\mathbf{k}_1),F(\mathbf{k}_2),\ldots,F(\mathbf{k}_M)]^T$ and $\mathbf{a}=[a_1,a_2,\ldots,a_M]^T$ are the data and coefficient column vectors, respectively, and $\mathbf{P}$ is the M by M square matrix with entries $P(\mathbf{k}_i-\mathbf{k}_j)$. Here the function $P(\mathbf{k})$ is the Fourier transform of the prior weighting function $p(\mathbf{r})$.

In many applications, calculating the matrix $\mathbf{P}$ is challenging, in particular if $p(\mathbf{r})$ is not available in closed form and the matrix elements cannot be computed from analytic expression. In addition, solving the system of Eq. (9) is costly, if not impractical, for large data sets. In contrast, the DPDFT does not require the matrix $\mathbf{P}$, and it is sufficient to provide $\mathbf{p}$ as a set of discrete numerical values.

For specificity we consider the two-dimensional problem in which $f(\mathbf{r})=f(x,y)$ and finitely many Fourier transform values of f are

$$F(\alpha_m,\beta_m) = \int\int f(x,y)\exp[-j(x\alpha_m + y\beta_m)]\mathrm{d}x\mathrm{d}y, \tag{10}$$

for $m=1,2,\ldots,M$. We approximate the two-dimensional integral in Eq. (10) using Riemann sums with $\mathrm{d}x \approx \Delta_x, \mathrm{d}y \approx \Delta_y$ for Δ_x,Δ_y being small enough,

$$F(\alpha_m,\beta_m) \approx \sum_{u=-U}^{U}\sum_{v=-V}^{V} f(u\Delta_x,v\Delta_y)\exp[-j(u\Delta_x\alpha_m + v\Delta_y\beta_m)]\Delta_x\Delta_y. \tag{11}$$

The object function $f(x,y)$ is assumed to reside entirely within the reconstructed image area, i.e., $f(x,y)=0$ for $|x|>U\Delta_x, |y|>V\Delta_y$. With the vectorization of the double sum in expression (11), it obtains a matrix equation $\mathbf{d}=\mathbf{Af}$. The vector $\mathbf{f}$ contains the values $f(u\Delta_x,v\Delta_y)$, and the matrix $\mathbf{A}$ has $\Delta_x\Delta_y$ times the complex exponentials in the double sum for its entries.

To incorporate prior knowledge, we write

$$\mathbf{Af} = \mathbf{AW}^{-1/2}\mathbf{W}^{1/2}\mathbf{f} = \mathbf{Bg}. \tag{12}$$

Instead of solving it in closed form, we calculate the minimum norm solution $\hat{\mathbf{g}}$ of $\mathbf{d}=\mathbf{Bg}$ using the ART. Beginning with the initial vector $\mathbf{g}^0$, the ART iterative step we set up to solve for $\hat{\mathbf{g}}$ in equation $\mathbf{d}=\mathbf{Bg}$ is given by

$$g_n^{k+1} = g_n^k + \frac{\bar{B}_{mn}(d_m - \sum_{i=1}^{N} B_{mi} g_i^k)}{\sum_{i=1}^{N} |B_{mi}|^2}, \tag{13}$$

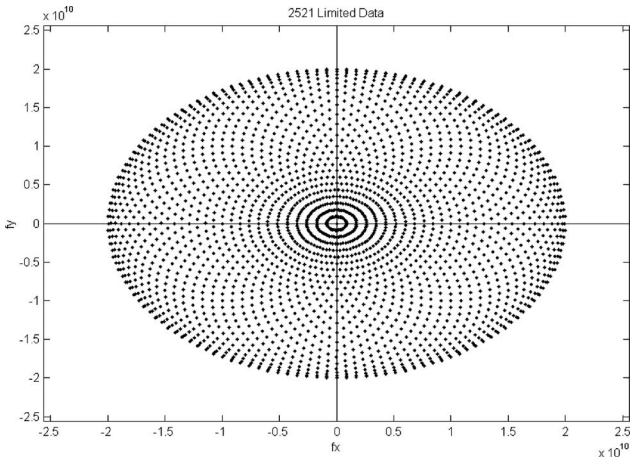

Fig. 1. Illustration of the Fourier space mapping of the simulated data.

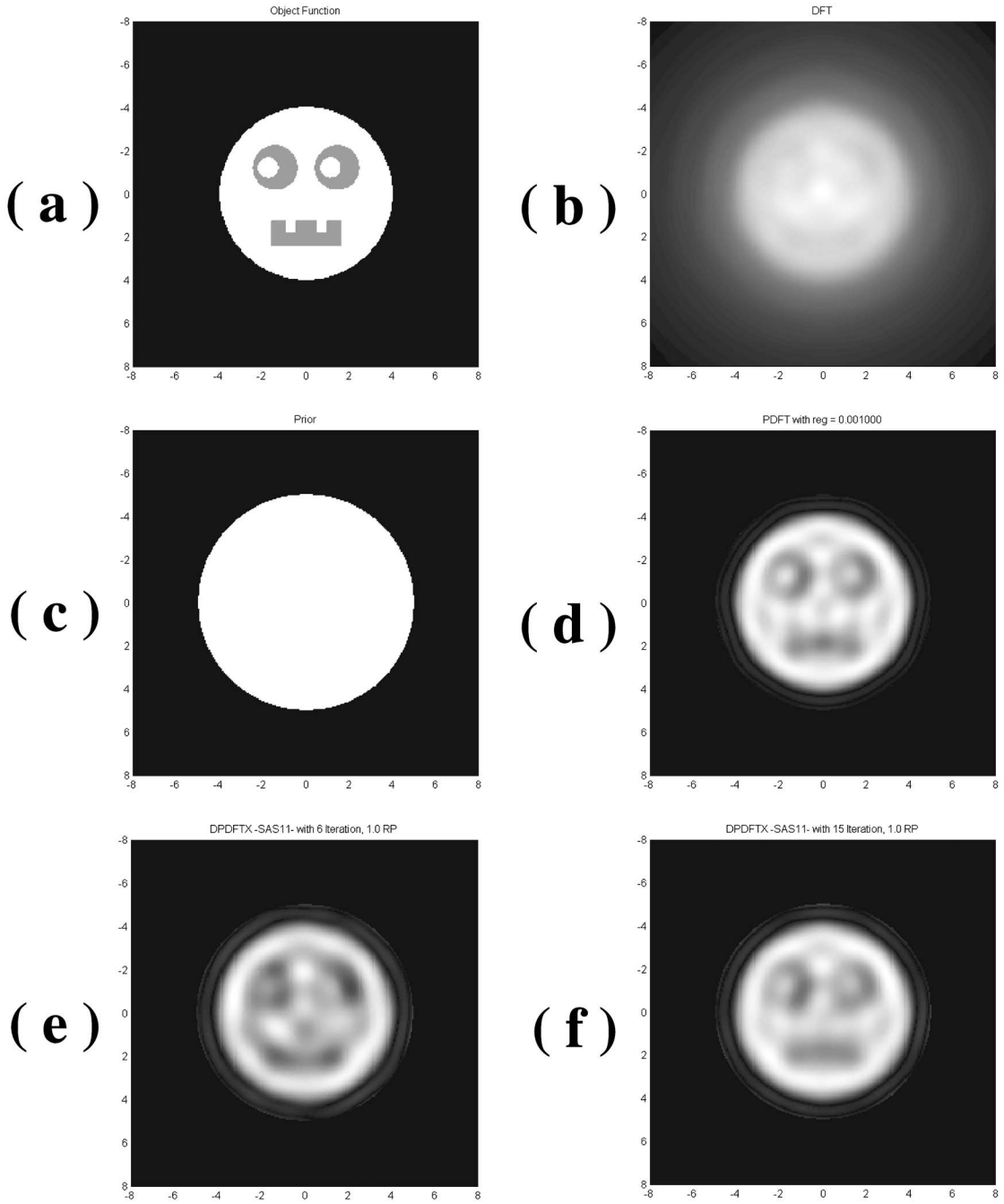

Fig. 2. Reconstruction of an object of compact support: (a) the object, (b) the discrete Fourier transform estimate, (c) circular flat top used as the prior function, (d) the PDFT estimate, (e) the DPDFT estimate after six iterations, (f) the DPDFT estimate after 15 iterations.

where $m=\mathrm{mod}(k,M)+1$. The ART algorithm in Eq. (13) converges to $\mathbf{g}^{\infty}$ for which $\|\mathbf{g}-\hat{\mathbf{g}}\|$ is minimized if there exist solutions for the system of equations $\mathbf{d}=\mathbf{Bg}$. Our estimate of $\mathbf{f}$ is then $\hat{\mathbf{f}}=\mathbf{W}^{-1/2}\hat{\mathbf{g}}$,

$$f_n^{k+1}=f_n^k+p_n\frac{\bar{A}_{mn}(d_m-\sum_{i=1}^{N}A_{mi}f_i^k)}{\sum_{i=1}^{N}p_i|A_{mi}|^2}. \tag{14}$$

The estimator of Eq. (14) is the so-called DPDFT.

3. CONVERGENCE OF THE ALGEBRAIC RECONSTRUCTION TECHNIQUE

The DPDFT requires finding the minimum weighted norm solution of an underdetermined system of linear equations. There are many ways to do this. In our simulations we have chosen to use the ART. We make no claims here about the best algorithm to use but merely wish to point out the improvements in ART that can be achieved through the use of relaxation, regularization, and attention to the ordering of the equations. It is important to note that in many applications of iterative methods in image reconstruction in which time is important,

only a few iterations of an iterative algorithm may be used. Therefore, how long it takes an algorithm to converge may be less significant than how good a job it does in the first few iterative steps.

The ART algorithm can be slow to converge when the equations are ordered in an unfavorable sequence. To improve it, there have been proposals for rearranging the order in which data are accessed. By randomizing the order in which data are accessed, or by optimizing the selection order in some sense, the convergence rate can be improved dramatically.[13–15] In addition, this slow convergence can also be improved by using the relaxation method,[16,17] which provides flexibility for choosing the new estimate at each iteration during the iterative process. To apply the relaxation in the ART, an adjustable parameter to the second term (projection) on the right-hand side of Eq. (13) is added. For the DPDFT, this step can be written as

$$f_n^{k+1} = f_n^k + \lambda^k p_n \frac{\bar{A}_{mn}(d_m - \sum_{i=1}^{N} A_{mi} f_i^k)}{\sum_{i=1}^{N} p_i |A_{mi}|^2}, \tag{15}$$

where λ^k is the relaxation parameter for the kth projection step.

To investigate the impact of rearranging and relaxation on the convergence performance of the DPDFT algorithm, we consider a two-dimensional problem of reconstructing an object function from its Fourier transform values. This demonstration particularly concentrates on one of our primary interests in developing the DPDFT algorithm for applications related to diffraction tomography. The data map in Fig. 1 is interpreted as the map of Fourier data that would be obtained from a bistatic radar experiment. The sampling points are equivalent to a radar frequency of 10 GHz, incident angles varying between 0° and 355° and scattered field angles ranging from 0° to 175°, both sampled with an increment of 5°. We emphasize, however, that only computed Fourier transform data were used to evaluate the convergence performance of the DPDFT under different environments; it was not necessary to take imperfections of an experimental data acquisition step into account.

For the reconstruction we used a circular prior function of a radius 5 cm [Fig. 2(c)]. The PDFT estimate in Fig. 2(d) shows better resolution than the DFT estimate in Fig. 2(b). The DPDFT estimate improves gradually at each iteration in accordance with the convergence characteristic of the ART.[17,18] The DPDFT estimate after six iterations is shown in Fig. 2(e), which is better resolved than the DFT estimate in Fig. 2(b); however, qualitatively the PDFT is superior. After 15 iterations the DPDFT estimate in Fig. 2(f) has improved significantly and shows similar quality as compared with the PDFT estimate.

For a quantitative evaluation, we take the root-mean-square error (RMSE) between the object function and its estimate as a measure of the accuracy of the image reconstruction:

$$RMSE = \sqrt{\frac{1}{N}\sum_{n=1}^{N} |o_n - r_n|^2}, \tag{16}$$

where N is the total number of pixels and o_n and r_n each represent the pixel value of the object and the image, respectively. For the example in Fig. 2, the RMSEs between the object and the PDFT estimate and between the object and the DPDFT estimate are shown in Fig. 3(a). The characteristic of the DPDFT estimate (solid curve) converges monotonically to the better solution as the number of iterations increases. In terms of computational efficiency the DPDFT avoids the costly creation and inversion of a 2521×2521 complex **P** matrix needed to compute the PDFT, but the DPDFT cannot obtain a resolution comparable to that of the PDFT estimate unless it completes 15 iterations or more. The iterative process of the DPDFT is typically subject to the problem of the slow convergence observed in Fig. 3(a), which may outweigh the

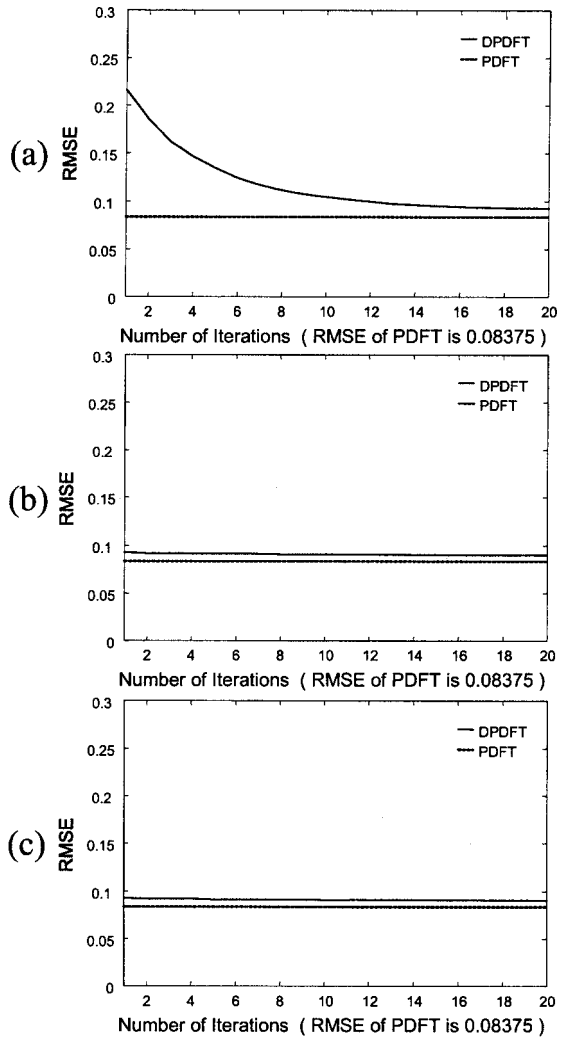

Fig. 3. RMSEs between the original and the reconstructed image for simulated noiseless Fourier data: (a) the RMSEs for the PDFT and the DPDFT after 1–20 iterations, (b) same as in (a) applying the RPS reordering, (c) same as in (a) applying the Herman–Meyer reordering.

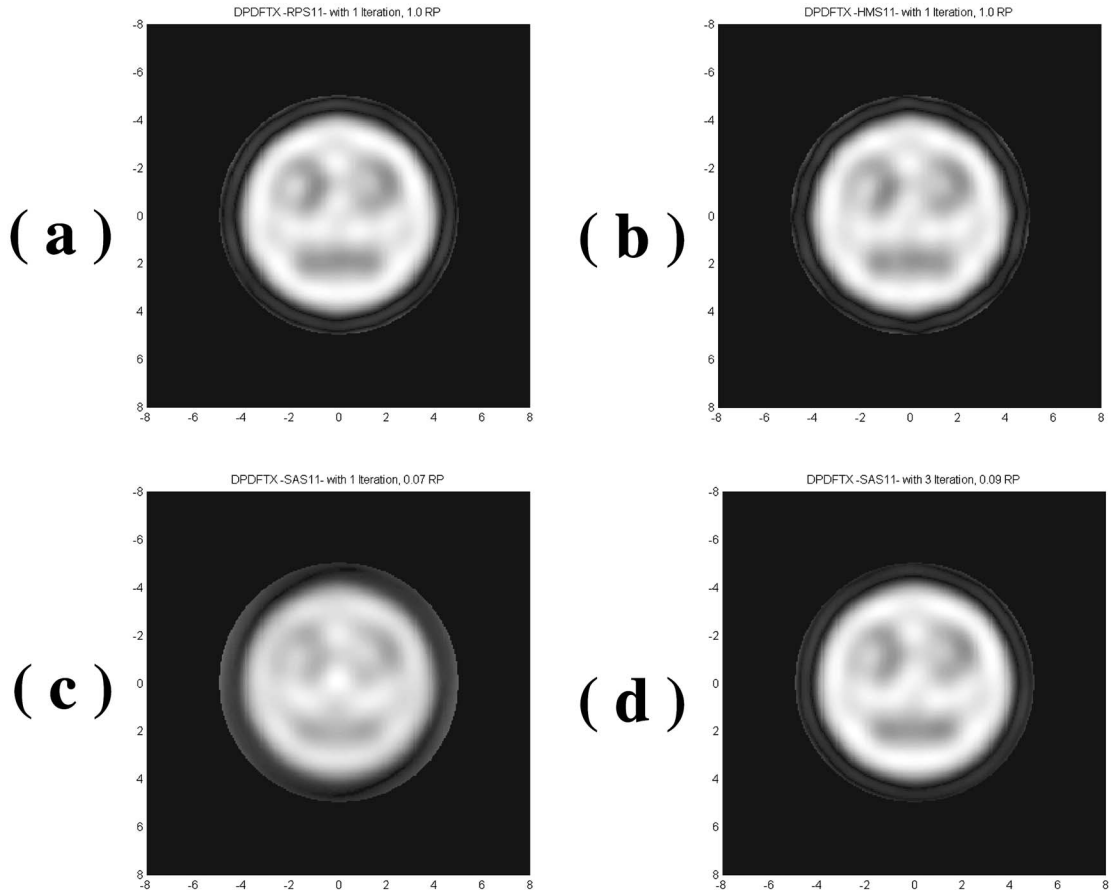

Fig. 4. Reconstruction of an object with compact support using the DPDFT with reordering and relaxation: (a) one-iteration DPDFT estimate with RPS reordering, (b) one-iteration DPDFT estimate with HMS reordering, (c) one-iteration DPDFT estimate with the relaxation parameter 0.07, (d) three-iteration DPDFT estimate with the relaxation parameter 0.09.

cost in time and memory associated with the setup and inversion of the **P** matrix.

For the same data used for the example in Fig. 2, we computed the image by implementing the random permutation scheme (RPS) and the Herman–Meyer scheme[14] (HMS) to adjust the data access order for the DPDFT. It is remarkable that the DPDFT estimate after one iteration with RPS reordering, in Fig. 4(a), and with HMS reordering, in Fig. 4(b), show resolution comparable to that of the DPDFT estimate after 15 iterations and without reordering, in Fig. 2(f). The quantitative improvement of the DPDFT by using either the RPS or the HMS reordering is illustrated in Figs. 3(b) and 3(c), respectively. As compared with that in Fig. 3(a), in Figs. 3(b) and 3(c) the convergence rate is improved dramatically, essentially approaching the final accuracy after about three iterations. However, in both cases the RMSE remains slightly above the value for the PDFT estimate. Since our implementation of the PDFT algorithms incorporates a Miller–Tikhonov regularization[19] step, the solution does not represent the minimum weighted norm approximation in a rigorous sense, and a small deviation between the reconstructions computed with DPDFT and PDFT is expected.

From the image in Fig. 4(d), we see that by choosing a relaxation parameter of 0.09 the DPDFT estimate requires only three iterations to improve to a resolution comparable to that of the DPDFT estimate after 15 iterations, but with no reordering and no relaxation [Fig. 2(f)]. If we apply one of the schemes to change the data access order simultaneously with applying the relaxation parameter, we obtain a solution comparable to the ones in Fig. 2(f) and 4(d) after only one iteration. In addition, we found that the use of reordering schemes extends the range for the relaxation parameter for which we obtain optimum performance (Fig. 5). In practice, this yields significantly higher stability, since the results obtained with the DPDFT are less sensitive to choice of the regularization parameter.

4. REGULARIZATION OF THE DISCRETE PRIOR DISCRETE FOURIER TRANSFORM

If the measured data are noisy, the iterative process of the DPDFT will typically converge to a poor solution of very large energy. For an explanation, we consider the same example in Fig. 2 but using noisy Fourier data. The noise sources considered here are simulated by Gaussian white noise. Leaving all other parameters unchanged, we find that the PDFT estimate must be regularized to recover a good estimate. For the PDFT algorithm with a Miller–Tikhonov regularization, the diagonal of the **P** matrix is multiplied with a factor $\epsilon=1+\kappa$, with $\kappa \ll 1$ typically. Among all computed PDFT results we found the regular-

ization value $\kappa=0.5$ to yield the smallest RMSE. The corresponding image estimate is shown in Fig. 6(a).

Likewise, in the case of noisy data the DPDFT cannot give a good estimate without regularization. The RMSEs between the object and the DPDFT estimates are shown in Fig. 7(a). The resolution of the DPDFT estimates improves gradually as the number of iterations increases. For more than eight iterations, however, the RMSE again increases. Both the DPDFT estimate after eight iterations [Fig. 6(b)] and the DPDFT estimate after 20 iterations [Fig. 6(c)] show poor resolution, which highlight the impact of noise on the performance of the DPDFT. The poor convergence due to noise can be addressed with suitable regularization methods. We now summarize a method for regularizing the DPDFT algorithm.

The underdetermined system of linear equations $\mathbf{Bg}=\mathbf{d}$ always has multiple solutions, even with noiseless data. Usually, the minimum norm solution is used to select a unique solution. It was shown that the ART converges to the minimum norm solution of the system of equations if it is implemented with a sequence of relaxation parameters $\lambda^k \in (0,2)$ converging to zero and the initial vector $\mathbf{f}^0$ is in $\mathbb{S}(\mathbf{A}^T)$.[17,18] Mathematically, $\mathbb{S}(\mathbf{A}^T)$ can be represented as

$$\mathbb{S}(\mathbf{A}^T)=\left\{\mathbf{v}|\mathbf{v}=\sum_{n=1}^{N}\alpha_n(\mathbf{A}^T)_{n-col},\ \text{for some arbitrary real numbers } \alpha_n\right\}, \quad (17)$$

where $(\mathbf{A}^T)_{n-col}$ denotes the nth column vector of the matrix $\mathbf{A}^T$. Typically, the origin is chosen as the initial vector, i.e., $\mathbf{f}^0=\mathbf{0}$. However, in the presence of noisy data, even this minimum norm solution can have a large norm and does not correspond to a useful reconstruction. Regularizing this scheme typically involves rejecting exact solutions of $\mathbf{Af}=\mathbf{d}$ and seeking instead a vector $\hat{\mathbf{f}}$, which minimizes the function $\|\mathbf{Af}-\mathbf{d}\|^2+\epsilon^2\|\mathbf{f}\|^2$, with $\epsilon>0$ being small.[20] The method due to the regularization uses the ART to solve the system of equations given in the matrix equation by

$$[\mathbf{A}\quad \epsilon\mathbf{I}]\begin{pmatrix}\mathbf{f}\\ \mathbf{v}\end{pmatrix}=\mathbf{d}. \quad (18)$$

For the ART iterative process of Eq. (18), we begin at $\mathbf{f}^0=\mathbf{0}$ and $\mathbf{v}^0=\mathbf{0}$, then the limit for its upper component $\mathbf{f}^\infty=\hat{\mathbf{f}}$. The iterative step can be represented as

$$f_n^{k+1}=f_n^k+p_n\bar{A}_{mn}\left(\frac{d_m-\sum_{i=1}^{N}A_{mi}f_i^k-\epsilon v_m^k}{\epsilon^2+\sum_{i=1}^{N}p_i|A_{mi}|^2}\right), \quad (19)$$

$$v_m^{k+1}=v_m^k+\epsilon\left(\frac{d_m-\sum_{i=1}^{N}A_{mi}f_i^k-\epsilon v_m^k}{\epsilon^2+\sum_{i=1}^{N}p_i|A_{mi}|^2}\right), \quad (20)$$

where

$$v_j^{k+1}=v_j^k \quad \text{for } j\neq \text{mod}(k,M)+1. \quad (21)$$

Then the reconstructed image is the limit of the sequence $\{\mathbf{f}^k\}$.

To illustrate this, we again consider the same example as used in Fig. 6, where the DPDFT did not converge significantly during the first eight iterations but diverged as the number of iterations increased. The result after eight iterations still looks poor as compared with the PDFT estimate in Fig. 6(a).

When we apply the regularization method [Fig. 6(d)], the DPDFT clearly converges after ten iterations, and the resulting image is comparable with the PDFT estimate in Fig. 6(e). The RMSEs as shown in Fig. 7(b) confirms the superior convergence of the DPDFT using regularization.

Further improvement is again observed by combining the regularization method with a changed data access order. The resulting RMSE values are plotted in Figs. 8(a) and 8(b). The convergence is significantly improved. Equally remarkable, the final RMSE value is slightly better than that of the PDFT estimate. The corresponding image estimates are shown in Figs. 6(e) and 6(f), which

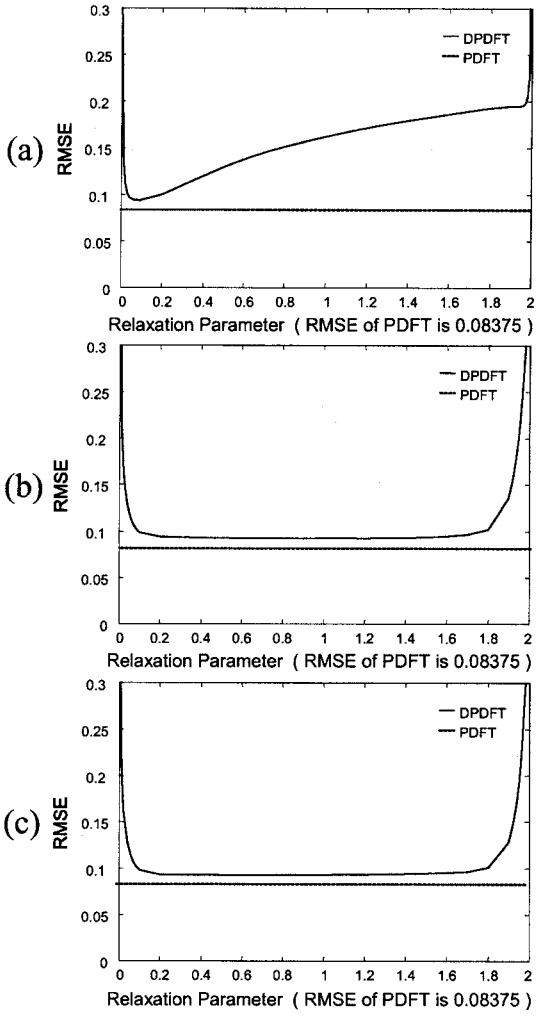

Fig. 5. Impact of the relaxation parameter on the RMSEs: (a) the RMSEs for the PDFT and the DPDFT after three iterations with no reordering, (b) same for the DPDFT after one iteration with RPS reordering, (c) same for the DPDFT after one iteration with HMS reordering.

confirm an image quality comparable with the PDFT estimate in Fig. 6(a) and the DPDFT estimate in Fig. 6(d).

5. CONCLUSION

We described the discrete implementation of the PDFT algorithm. The PDFT algorithm and its discrete counterpart, the DPDFT algorithm, are typically used to compute image estimates from projection data. Both algorithms allow one to incorporate prior knowledge about the imaging problem to improve the reconstructed image.

The DPDFT algorithm was implemented primarily as a substitute for the well-explored PDFT algorithm, since it does not require the inversion of the **P** matrix. If the optimum reconstruction can be obtained with a few iterations of the DPDFT, this invariably provides a speedup as compared with the implementation of the PDFT algorithm, which increases with the size of the data set. However, the more important application of the DPDFT is with respect to data sets that are too large to allow for the inversion of the corresponding **P** matrix.

In addition, we emphasize that the DPDFT algorithm

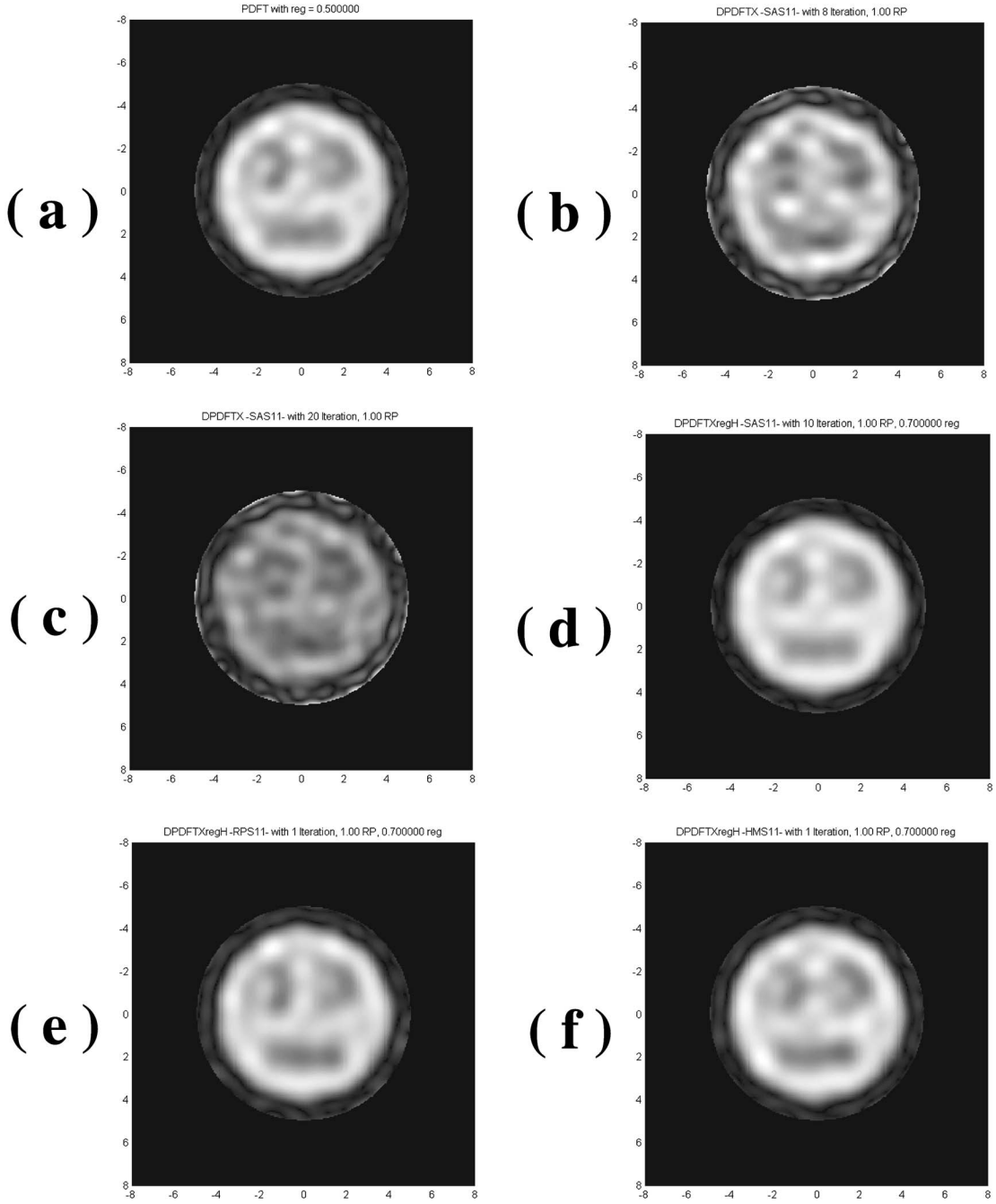

Fig. 6. Reconstruction of an object of compact support from the noisy data: (a) the PDFT estimate with regularization value of $\kappa=0.5$, (b) the DPDFT estimate after eight iterations, (c) the DPDFT estimate after 20 iterations, (d) the DPDFT estimate after ten iterations with regularization value of $\epsilon=0.7$, (e) the DPDFT estimate after one iteration with regularization value of $\epsilon=0.7$ and RPS reordering, (f) the DPDFT estimate after one iteration with regularization value of $\epsilon=0.7$ and HMS reordering.

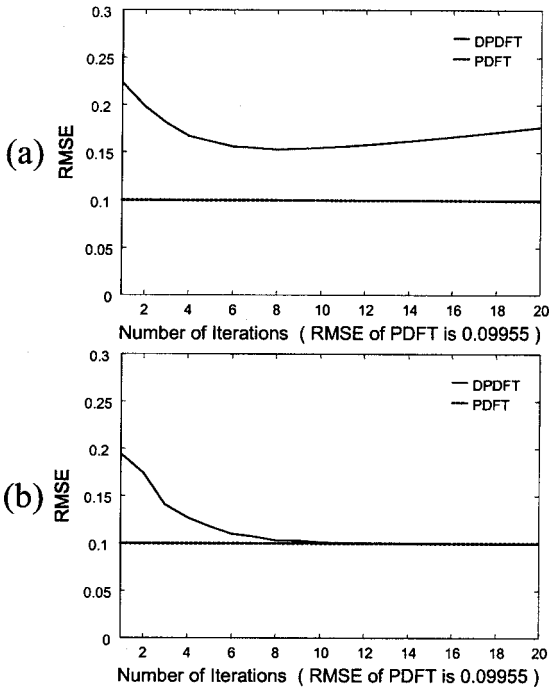

Fig. 7. RMSEs between object and image computed from simulated noisy data: (a) the DPDFT estimate without regularization, (b) the DPDFT estimate with regularization value of $\epsilon=0.7$.

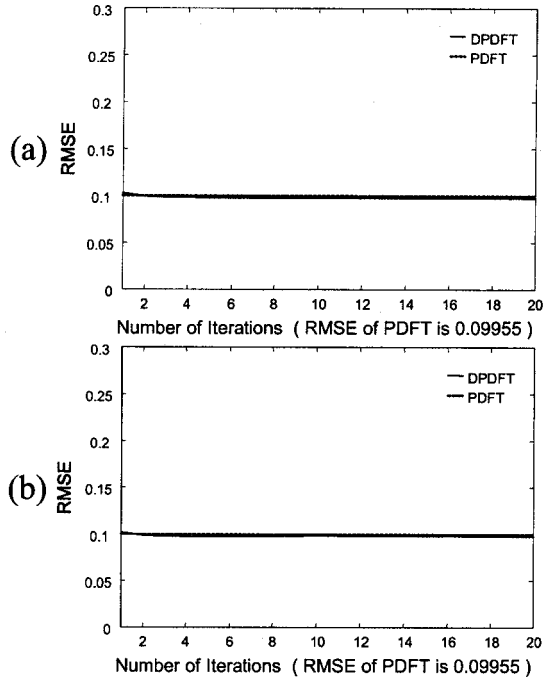

Fig. 8. RMSEs between object and image for simulated noisy data: (a) RPS reordering and regularization value of $\epsilon=0.7$, (b) HMS reordering and regularization value of $\epsilon=0.7$.

eliminates the need to compute the Fourier transformation of the prior in order to obtain a reconstruction of the object. This property is particularly useful if the prior is not given in analytic form but is the result of a preprocessing step and is only available in discrete form. In this case the DPDFT algorithm is the method of choice to obtain a constraint image estimate of the object. It is noted, however, that even if the prior is available in analytic form the computation of the P matrix can contribute significantly to the computational burden of the PDFT algorithm, and the DPDFT provides a more efficient use of the prior information.

In our examples, the DPDFT was implemented using the ART algorithm, although this is not essential, and we make no assertions for or against the ART. We demonstrated that the convergence speed can be improved by reordering, which was successfully applied to ART-related reconstruction schemes in the past. In particular, we investigated changing the access order of individual elements of the system of linear equations that needs to be solved. Independently of the access order scheme chosen, we found significant improvement of the convergence.

For noisy data it proved necessary to implement a suitable regularization method. Again, the behavior of the DPDFT algorithm proved sufficiently similar to previously described variants of the ART to adapt a known regularization scheme for use with the DPDFT algorithm. Our results show that this allows us to address noise-related imaging problems effectively.

Authors' e-mail addresses: hmshieh@fcu.edu.tw, Charles_Byrne@uml.edu, Markus.E.Testorf@Dartmouth.edu, and mafiddy@uncc.edu.

REFERENCES

1. C. L. Byrne and R. M. Fitzgerald, "Reconstruction from partial information, with applications to tomography," SIAM J. Appl. Math. **42**, 933–940 (1982).
2. C. L. Byrne, R. M. Fitzgerald, M. A. Fiddy, T. J. Hall, and A. M. Darling, "Image restoration and resolution enhancement," J. Opt. Soc. Am. **73**, 1481–1487 (1983).
3. C. L. Byrne and R. M. Fitzgerald, "Spectral estimators that extend the maximum entropy and maximum likelihood methods," SIAM J. Appl. Math. **44**, 425–442 (1984).
4. C. L. Byrne and M. A. Fiddy, "Image as power spectral; reconstruction as a Wiener filter approximation," Inverse Probl. **4**, 399–409 (1988).
5. H. M. Shieh, C. L. Byrne, and M. A. Fiddy, "Image reconstruction: a unifying model for resolution enhancement and data extrapolation. Tutorial," J. Opt. Soc. Am. A **23**, 258–266 (2006).
6. C. L. Byrne, *Signal Processing: A Mathematical Approach* (AK Peters, 2005).
7. S. Kaczmarz, "Angenaherte auflosung von system linearer gleichungen," Bull. Int. Acad. Pol. Sci. Lett., Cl. Sci. Math. Nat., Ser. A **35**, 355–357 (1937).
8. R. Gordon, R. Bender, and G. T. Herman, "Algebraic reconstruction techniques (ART) for three-dimensional electron microscopy and x-ray photography," J. Theor. Biol. **29**, 471–481 (1970).
9. K. Tanabe, "Projection method for solving a singular system of linear equations and its applications," Numer. Math. **17**, 203–214 (1971).
10. R. Gordon, "A tutorial on ART," IEEE Trans. Nucl. Sci. **NS-21**, 78–93 (1974).
11. G. T. Herman and A. Lent, "Iterative reconstruction algorithms," Comput. Biol. Med. **6**, 273–294 (1976).
12. G. T. Herman and H. K. Tuy, "Image reconstruction from projections: an approach from mathematical analysis," in *Basic Methods of Tomography and Inverse Problems*., P. C. Sabatier, ed. (Hilger, 1987), pp. 1–124.

13. G. T. Herman, *Image Reconstruction from Projections: The Fundamentals of Computerized Tomography* (Academic, 1980).
14. G. T. Herman and L. B. Meyer, "Algebraic reconstruction techniques can be made computationally efficient," IEEE Trans. Med. Imaging **12**, 600–609 (1993).
15. H. Guan and R. Gordon, "A projection access order for speedy convergence of ART (algebraic reconstruction technique): a multilevel scheme for computed tomography," Phys. Med. Biol. **39**, 2005–2022 (1994).
16. G. T. Herman, "A relaxation method for reconstructing objects from noisy X-rays," Math. Program. **8**, 1–19 (1975).
17. G. T. Herman, A. Lent, and P. H. Lutz, "Relaxation methods for image reconstruction," Commun. ACM **21**, 152–158 (1978).
18. M. R. Trummer, "Reconstructing pictures from projections: on the convergence of the ART algorithm with relaxation," Computing **26**, 189–195 (1981).
19. M. Bertero and P. Boccacci, *Introduction to Inverse Problems in Imaging* (Institute of Physics, 1998).
20. P. Eggermont, G. T. Herman, and A. Lent, "Iterative algorithms for large partitioned linear systems, with applications to image reconstruction," Linear Algebr. Appl. **40**, 37–67 (1981).